



Essential role of microfibrillar-associated protein 4 in human cutaneous homeostasis and in its photoprotection

SUBJECT AREAS:
PATTERN FORMATION
DEVELOPMENT
BIOMARKERS
EXTRA-CELLULAR MATRIX

Shinya Kasamatsu¹, Akira Hachiya¹, Tsutomu Fujimura¹, Penkanok Sriwiriyant², Keiichi Haketa¹, Marty O. Visscher³, William J. Kitzmiller⁴, Alexander Bello⁵, Takashi Kitahara¹, Gary P. Kobinger⁵ & Yoshinori Takema¹

Received
5 August 2011

Accepted
8 November 2011

Published
22 November 2011

Correspondence and requests for materials should be addressed to A.H. (hachiya.akira@kao.co.jp)

¹Biological Science Laboratories, Kao Corporation, Haga, Tochigi, 321–3497, Japan, ²Department of Biomedical Engineering, University of Cincinnati, Cincinnati, OH 45267, USA, ³Division of Neonatology and Skin Sciences Institute, Cincinnati Children's Hospital Medical Center, Cincinnati, OH, 45229, USA, ⁴Department of Surgery, University of Cincinnati, Cincinnati, OH, 45267, USA, ⁵Special Pathogens Program, National Microbiology Laboratory, Public Health Agency of Canada, Department of Medical Microbiology, University of Manitoba, Winnipeg, Manitoba R3E 3R2, Canada.

UVB-induced cutaneous photodamage/photoaging is characterized by qualitative and quantitative deterioration in dermal extracellular matrix (ECM) components such as collagen and elastic fibers. Disappearance of microfibrillar-associated protein 4 (MFAP-4), a possible limiting factor for cutaneous elasticity, was documented in photoaged dermis, but its function is poorly understood. To characterize its possible contribution to photoprotection, MFAP-4 expression was either augmented or inhibited in a human skin xenograft photodamage murine model and human fibroblasts. Xenografted skin with enhanced MFAP-4 expression was protected from UVB-induced photodamage/photoaging accompanied by the prevention of ECM degradation and aggravated elasticity. Additionally, remarkably increased or decreased fibrillin-1-based microfibril development was observed when fibroblasts were treated with recombinant MFAP-4 or with MFAP-4-specific siRNA, respectively. Immunoprecipitation analysis confirmed direct interaction between MFAP-4 and fibrillin-1. Taken together, our findings reveal the essential role of MFAP-4 in photoprotection and offer new therapeutic opportunities to prevent skin-associated pathologies.

Skin, the outermost barrier of the body, plays an important role in protection against environmental assaults including UV radiation which has been documented to be associated with the increased incidence of photoaging and photocarcinogenesis, in part due to the marked destruction of the stratospheric ozone layer over the past decades^{1–3}. Photodamage/photoaging is a term describing the time-dependent changes that occur in chronically sun-exposed skin which appears to be an acceleration of the intrinsic aging process that occurs even in sun-protected skin⁴. Skin photodamage/photoaging has been reported to be physiologically correlated with several alterations including the increased disorganization of elastic fibers and the reduction of collagens in the dermal ECM^{5–12} as well as the increased levels of keratins 6 and 16 and the deterioration of keratin intermediate filaments in the epidermis^{13–16}. Elastic fibers, as well as collagen fibers, are components of the dermal ECM that primarily account for the fibrous mechanism(s) controlling cutaneous elasticity^{5,6,17,18}. In addition to the degeneration of elastic fibers in chronologically and/or photoaged skins that have been reported to stem from increased activities of matrix metalloproteinase (MMP)-12 and/or elastase^{19–22}, the accumulation of dystrophic elastotic material in the reticular dermis, referred to as solar elastosis, is also commonly observed in photoaged skin^{23–25}. With regard to the incidence of solar elastosis, UVB radiation has been demonstrated both *in vivo* and *in vitro* to up-regulate tropoelastin gene expression and protein abundance in fibroblasts and in keratinocytes, which results in an aberrant accumulation of dermal elastic fibers and elastin content^{6,9,11,12,26}. However, the mechanisms underlying the alteration of elastic fibers in photoaged skin, including their production, accumulation and degradation, have not been fully characterized to date.

Elastic fibers, in spite of their lower abundance compared to collagen fibers, are larger structures of the ECM that control the elastic properties of connective tissues which consist of two major components, microfibrils and tropoelastin. One of the major structural constituents of microfibrils is fibrillin-1, a large (~350 kDa) cysteine-rich glycoprotein, whose amount has been reported to be significantly decreased in tissues and in cells from



patients with Marfan syndrome who demonstrate ocular, cardiovascular, and skeletal abnormalities^{27,28}. In addition, the fibrillin-1 monomer has been documented to be assembled both linearly and laterally to form the frame of microfibrils²⁹, followed by its association with various other proteins, including latent TGF- β -binding proteins (LTBPs), fibulins, microfibril associated glycoproteins and elastin microfibril interface located protein-1, to produce mature microfibrils³⁰. On the other hand, tropoelastin, a 60–70 kDa protein that has lysine-containing cross-linking and hydrophobic domains, is subjected to a process of well-regulated self-aggregation called coacervation that is induced by specific interactions of each hydrophobic domain under optimized conditions³¹. Coacervation can be stimulated by an increase in temperature and is thought to be an important prerequisite process for cross-linking^{32–34}. It was proposed that tropoelastin binds microfibrils followed by coacervation to be cross-linked by lysyl oxidase (LOX)²⁹.

Apart from microfibrils and tropoelastin, MFAP-4 has been considered as a human homologue of 36 kDa microfibril-associated glycoprotein (MAGP-36) due to its high level of an Arg-Gly-Asp (RGD) sequence homology, its fibrinogen-like domain and its similar molecular weight, which was initially discovered in the porcine aorta and has been detected in the elastic tissue of various animals^{35–39}. An immunohistochemical study demonstrated that MAGP-36, which is localized around elastic fibers in the rat aorta and is rich in elastin-associated microfibrils, had disappeared in photoaged dermis and could be found in the accumulation of disintegrated elastic fibers in the lesional skin of pseudoxanthoma elasticum, an elastin-related disorder⁴⁰. That report strongly suggested that MAGP-36 is a microfibrillar-associated protein, although little is known about its role(s) in human elastic tissues.

In this study, a human skin xenograft model in combination with a lentiviral vector was used to assess the role of MFAP-4 in human skin. Despite that a lot of studies on skin photoaging have been conducted using animal models and human skin substitutes, it has been suggested that these results may be misleading because of the differences in inferior architectures, such as the relative thin epidermal layer and compromised barrier function between genuine human skin and the models and that the use of actual human skins or human skin xenografts is more appropriate for the study on skin photoaging. Therefore human xenografted photodamage/photoaging model which had been previously established was introduced in this study¹⁶. Our results demonstrate for the first time that MFAP-4 plays a critical role in fibrillin-1-based microfibril assembly and is associated with elastic fiber formation, resulting in the protection of the skin photodamage/photoaging.

Results

Abundance of MFAP-4 is significantly decreased both in extrinsically photoaged skin and in intrinsically aged skin. In order to characterize the possible function of MFAP-4 to protect skin from photodamage and/or aging, expression of MFAP-4 was evaluated in a photoaging skin model induced by repeated UVB exposure and in intrinsically aged skin. Human skin xenografted onto severe combined immunodeficiency (SCID) mice was exposed to 1 to 2 minimal erythema dose (MED) UVB radiation for 6 weeks (wks) and total RNAs were extracted for transcript expression analysis. Skin punch biopsies from the ventral upper arms of healthy Caucasian females in their twenties and fifties were also used for total RNA extraction. Quantitative RT-PCR analysis showed that expression of MFAP-4 was significantly lower in the photoaging skin model, which is consistent with a previous report⁴⁰ (Fig. 1a). Similarly, expression of MFAP-4 was also significantly impaired in intrinsically aged skin (Fig. 1b), suggesting a potential role for MFAP-4 in protection against cutaneous aging. In consistent with mRNA transcript evaluation, immunohistochemical comparison using the dermis at the ventral

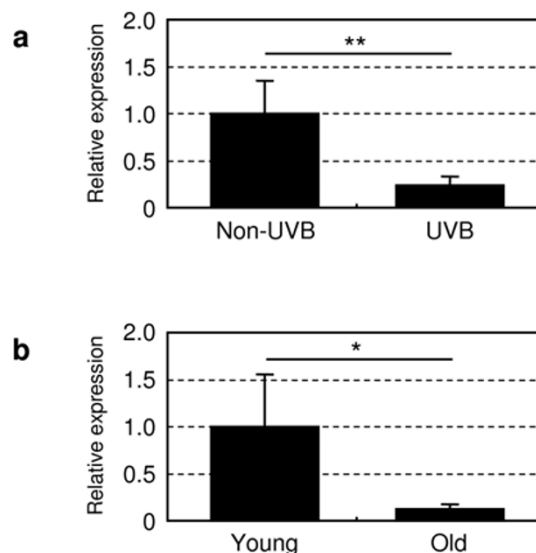


Figure 1 | Expression of MFAP-4 transcripts in photodamaged/photoaged and in intrinsically aged skins. Quantitative RT-PCR analysis of MFAP-4 in human skin was performed. (a) The expression of MFAP-4 in xenografted human skin after repeated UVB irradiations with 1 to 2 MED for 6 wks was normalized to the expression of the ribosomal protein, RPLP0, and the relative value compared to the non-irradiated control is shown. (b) MFAP-4 expression in human skin punch biopsies at the ventral area of upper arms from young (twenties) and old (fifties) Caucasian women. The results normalized by RPLP0 expression are presented. Values reported represent means \pm SD. * $p < 0.05$, ** $p < 0.01$.

upper arms (sun-protected areas) of Caucasian skin specimens clearly demonstrated that MFAP-4 protein localisation detected over the dermis in their thirties was remarkably diminished in their sixties. Interestingly its protein levels were found to be almost abolished in the dermis at the dorsal lower arms (sun-exposed areas) of the donors in their sixties (Fig. 2).

Over-expression of MFAP-4 protects the skin from chronic UVB-induced photodamage. Following the observation of the down-regulation of MFAP-4 expression both in photodamaged/photoaged skin and in intrinsically aged skin, a lentiviral vector over-expressing MFAP-4 was subepidermally injected into the xenografted skin to investigate whether cutaneous over-expression of MFAP-4 prevents photodamage/photoaging. MFAP-4 expression in the skin treated with a lentiviral vector encoding MFAP-4 was confirmed to remain higher than in skin over-expressing a control reporter gene by Western blotting analysis before and after UVB irradiation for 4 wks (data not shown). In addition, immunohistochemical analysis using xenografted skin just after UVB irradiation for 8 wks demonstrated the even higher protein contents of MFAP-4 in the skin treated with a lentiviral vector encoding MFAP-4 than in the skin over-expressing a control reporter gene (Fig. 3b), suggesting that higher expression of MFAP-4 was maintained during the experimental period.

During the course of chronic UVB irradiation, *en face* representative images of xenografted skin demonstrated that furrow formation was induced gradually in the control reporter gene-transduced skin (Fig. 3c). This was in agreement with the quantitative analyses of skin surface roughness and skin elasticity which demonstrates significant increases in both parameters (Sa and Sz) at 10 and 14 wks (after UVB exposure for 4 and 8 wks) in the repeated UVB-exposed skin compared to the non-UVB irradiated control transfected with the control reporter gene (Fig. 3d). Additionally, the impaired value of pure elasticity (Ur/Ue) was also recorded at 10 wks (after UVB exposure for 4 wks) (Fig. 3e). The increase in skin surface roughness was kept for at least 6 wks after the final UVB irradiation. In contrast, the

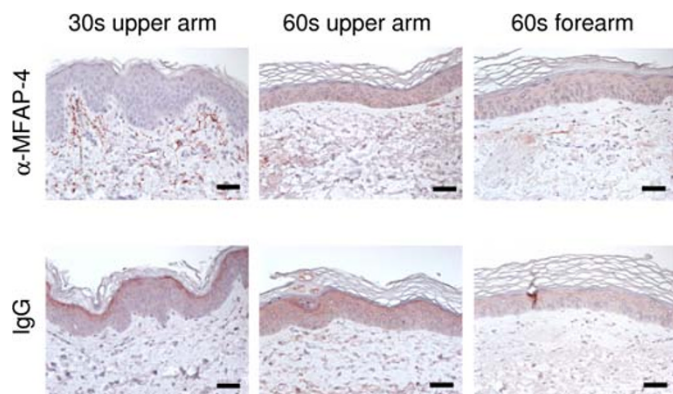


Figure 2 | More decreased deposition of MFAP4 in photodamaged/ photoaged skin than intrinsically aged skin. Immunohistological staining with rabbit polyclonal anti-human MFAP-4 and normal rabbit control IgG was conducted on paraffin embedded sections of biopsied skin specimens. They were from the ventral upper arm of the donors in their thirties and sixties, or from the dorsal lower arms of the donors in their sixties. Scale bars = 50 μ m.

UVB-induced surface roughness was found to be remarkably diminished in skin over-expressing *MFAP-4* according to *en face* images and skin surface roughness parameters (Sa and Sz) demonstrating significantly lower values compared to those in UVB-exposed skin over-expressing the control reporter gene (Fig. 3c, d). Consistently, the

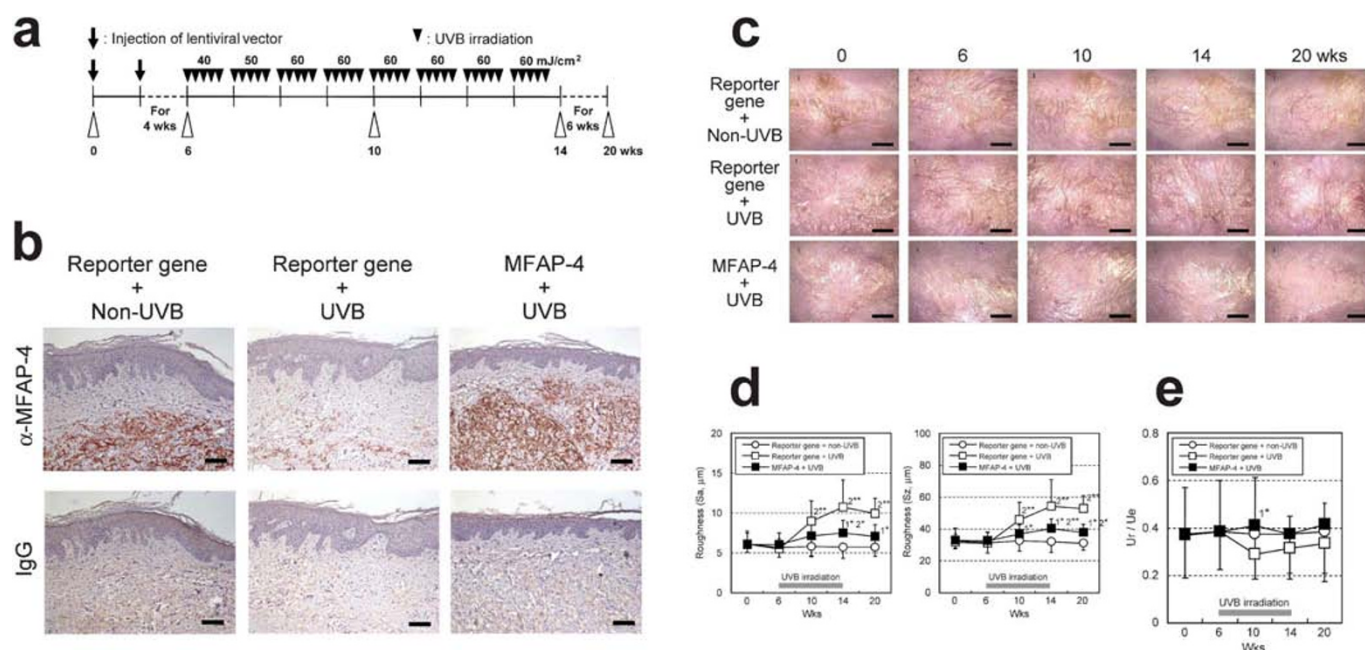


Figure 3 | Protection of skin from UVB-induced photodamage by enhancement of *MFAP-4* expression. (a) Lentiviral vectors to over-express *MFAP-4* or a control reporter gene were intradermally administered to human xenografted skin twice with a week interval, subjected to continuous UVB irradiations at 1 to 2 MED for 8 wks as indicated. (b) Immunohistological staining with rabbit polyclonal anti-human MFAP-4 and normal rabbit control IgG was performed on paraffin embedded sections from non-exposed skin with a control reporter gene over-expression, a control reporter gene-transduced skin with UVB irradiation for 8 wks and *MFAP-4*-over-expressed skin with repetitive UVB irradiation for 8 wks. Scale bars = 100 μ m. (c) *En face* representative images of xenografted skin were captured at 0 (before the lentiviral administration), 6 (before the UVB irradiation), 10, 14 (just after the completion of continuous UVB exposures) and 20 wks (6 wks after the final UVB irradiation) using a hand-held microscope. The non-UVB irradiated control with a control reporter gene over-expression, the long-term UVB-irradiated skin with a control reporter gene over-expression and *MFAP-4*-over-expressed skin with repetitive UVB exposure are shown at the top, middle and bottom, respectively. Scale bars = 3 mm. (d) Skin profilometry of replicas was utilized to evaluate surface roughness using arithmetic mean roughness (Sa) and mean peak to valley height (Sz) at the indicated time points. The values reported represent means \pm SD. * p <0.05, ** p <0.01. 1; vs the values of the UVB-irradiated control with a control reporter gene over-expression. 2; vs the values of the non-irradiated control with a control reporter gene over-expression. (e) Skin elasticity was evaluated using a Cutometer SEM575 at the same time points as the assessments of skin surface roughness. Ur/Ue represents pure elasticity ignoring creep. The values reported represent means \pm SD. * p <0.05. 1; vs the values of the UVB-irradiated control with a control reporter gene over-expression.

value of Ur/Ue was significantly higher in skin over-expressing *MFAP-4* than in UVB-exposed skin over-expressing the control reporter gene at 10 wks (after UVB exposure-driven for 4 wks) (Fig. 3e), adding more evidences to the protective role of *MFAP-4* against UVB-induced photodamage/photoaging.

MFAP-4 is essential to elastic fiber assembly. The finding of the protective role of *MFAP-4* led us to examine the impact of *MFAP-4* on elastic fiber formation. Fig. 4a shows Luna staining of human skin xenografted on SCID mice. Elastic fibers in the control reporter gene-transfected skin exposed to UVB for 8 wks were remarkably diminished compared to those in non-UVB exposed skin over-expressing the control reporter gene. On the other hand, skin treated with the *MFAP-4*-over-expressing vector was protected from the repetitive UVB exposure-driven degradation of elastic fibers. Interestingly, the UVB induced up-regulation of MMP-12 activity, which has been reported to be secreted from dermal fibroblasts to deteriorate elastic fibers^{19–22}, was significantly suppressed in the skin by over-expression of *MFAP-4* (Fig. 4b).

Following that *in vivo* analysis, further detailed analysis on the mechanisms underlying the elastic fiber assembly promoted by *MFAP-4* was performed using normal human dermal fibroblasts (NHDFs). NHDFs treated with a non-specific siRNA in the presence or absence of human recombinant *MFAP-4* or NHDFs treated with a siRNA specific for *MFAP-4* were cultured for 8 days to allow NHDFs to assemble elastic fibers. After confirmation of the marked reduction of *MFAP-4* transcript and protein levels by treatment with the *MFAP-4*-specific siRNA (Fig. 5a, b), immunohistochemical analysis

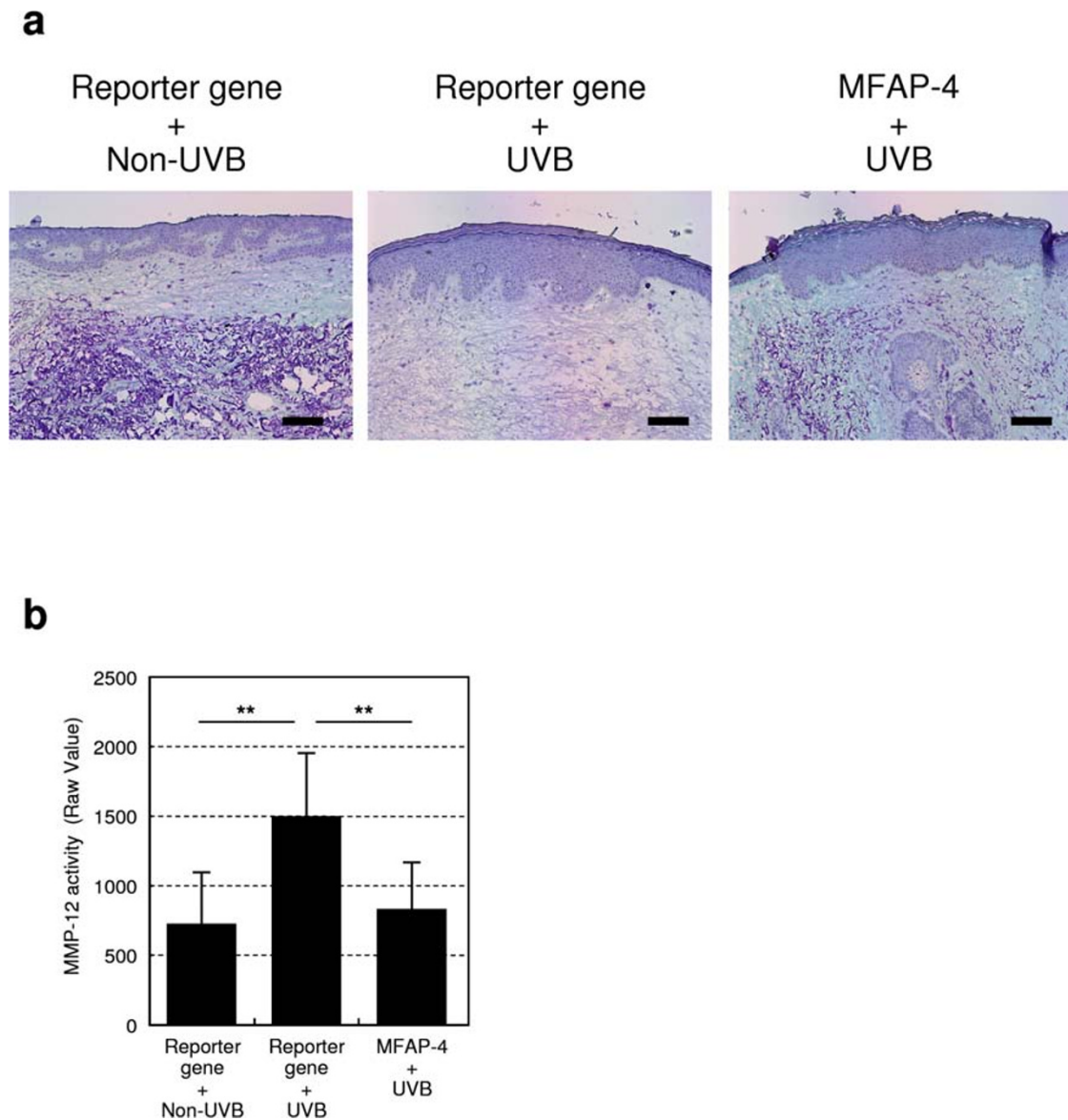


Figure 4 | Effect of *MFAP-4* over-expression on the UVB-induced increase in MMP-12 activity. (a) Luna staining was performed to evaluate the role of *MFAP-4* in the protection of elastic fibers using paraffin-embedded sections from non-exposed skin with a control reporter gene over-expression, a control reporter gene-transduced skin with UVB irradiation for 8 wks and *MFAP-4*-over-expressed skin with repetitive UVB irradiation for 8 wks. Scale bars = 100 μ m. (b) MMP-12 activities in xenografted human skins treated with lentiviral vectors encoding a control reporter gene with or without UVB irradiation for 8 wks and UVB-exposed skin with *MFAP-4* over-expression were evaluated using fluorescent-tagged MMP-12 substrate as detailed in the Methods. The values reported represent means \pm SD. ** $p < 0.01$; vs the value in UVB-exposed skin with a control reporter gene over-expression.

with anti-human tropoelastin and anti-human fibrillin-1 antibodies was performed. The association of tropoelastin and fibrillin-1, which are both essential to generate elastic fibers, was found to be reduced on the cells with suppressed *MFAP-4* protein contents compared to cells treated with a non-specific siRNA (Fig. 5c), whereas total protein levels of fibrillin-1 in the supernatant of cultured NHDFs was not changed by the administration with the *MFAP-4*-specific siRNA (Fig. 5b). On the other hand, increases in their assemblies were observed following treatment with human recombinant *MFAP-4*, which resulted in the enhancement of elastic fiber assembly. Consequent to the diminished organization of elastic fibers by the *MFAP-4*-specific siRNA, the levels of the MMP-12 transcript expression and protein was stimulated by the repression of *MFAP-4* expression (Fig. 5d, e). To confirm the role of *MFAP-4* in the acceleration of elastic fiber formation, NHDFs were cultured for 8 days in non-fetal bovine serum (FBS) starved conditions with or without human recombinant *MFAP-4*. Immunohistochemical staining of

elastic fiber components demonstrated that the colocalisation of tropoelastin and fibrillin-1 in NHDFs was close to the limit of detection in control cells not treated with human recombinant *MFAP-4*, whereas their protein abundance following treatment with human recombinant *MFAP-4* was enhanced (Fig. 5f).

Additionally, to elucidate which cellular components interact directly or indirectly with *MFAP-4*, concentrated supernatants from NHDFs were immunoprecipitated with an anti-*MFAP-4* antibody, followed by Western blotting analysis with anti-fibrillin-1 or anti-tropoelastin antibodies. Corresponding signals were detected using an antibody specific for fibrillin-1 (Fig. 6a), whereas no signal was observed when an anti-tropoelastin antibody was used (data not shown). Furthermore, the colocalisation of *MFAP-4* with fibrillin-1 was confirmed in NHDFs transfected with a non-specific siRNA by immunocytochemical analysis (Fig. 6b). Intriguingly, decreased signal of fibrillin-1 was observed in NHDFs transfected with an *MFAP-4*-specific siRNA synchronized with the depletion of *MFAP-4*,

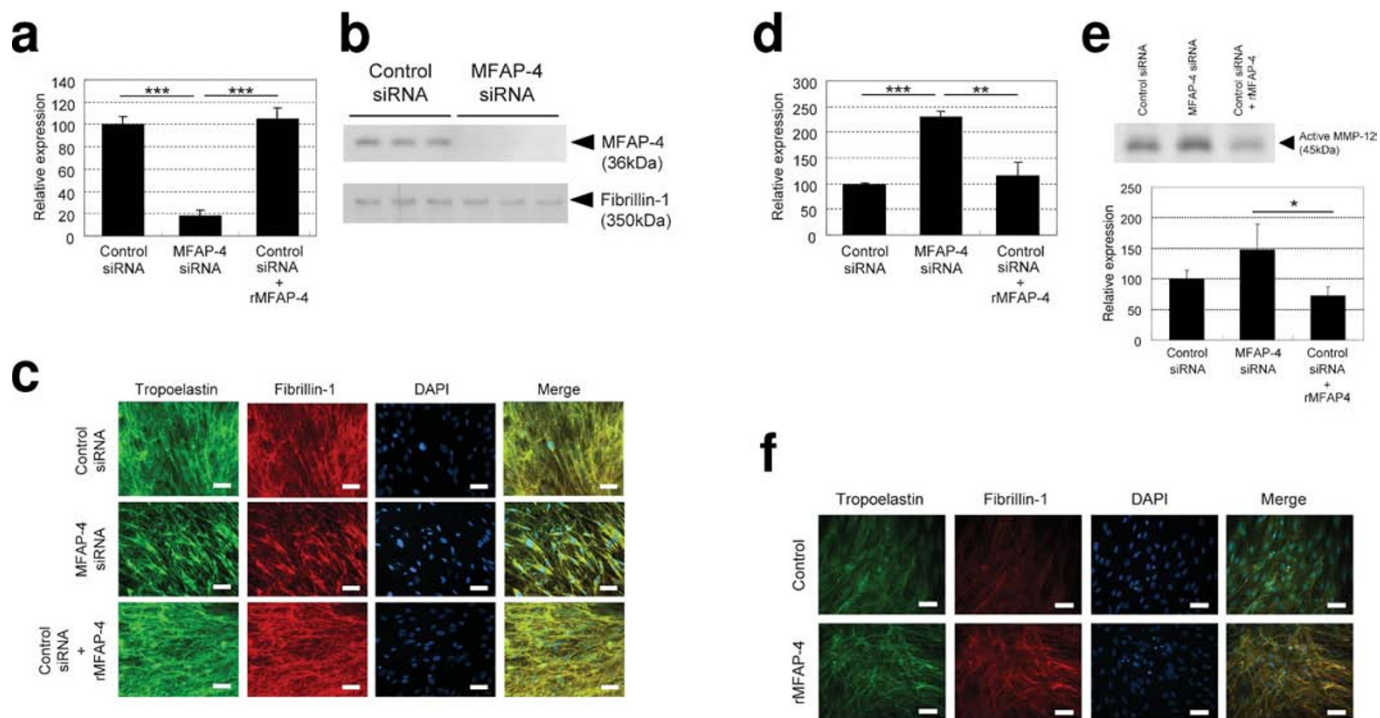


Figure 5 | MFAP-4 is essential to the assembly of elastic fibers. NHDFs were transfected with siRNAs for non-specific sequences (Control) or MFAP-4 twice during the culture for 8 days. Control siRNA-transfected cells were treated with or without 10 nM human recombinant MFAP-4 during the culture. (a) Quantitative RT-PCR analysis was performed with *MFAP-4*-specific *TaqMan* Gene Expression Assays after the reverse transcription of total RNAs from cultured NHDFs. The mRNA expression of the target gene was normalized against the expression of *GAPDH* mRNA and is relatively presented. The values reported represent means \pm SD. *** $p < 0.001$. (b) Western blotting analysis with antibodies specific for MFAP-4 or fibrillin-1 was conducted to confirm the impact of MFAP-4 silencing on their protein abundance using the supernatants from cultured NHDFs. (c) Immunofluorescence staining was performed with an anti-human tropoelastin antibody (green) and an anti-human fibrillin-1 antibody (red). Nuclear staining (DAPI) and merged images are also shown in the diagram. Scale bars = 50 μ m. (d) Quantitative RT-PCR analysis of the *MMP-12* mRNA expression in cultured NHDFs was performed as described in the legend of Fig. 5a. The values reported represent means \pm SD. *** $p < 0.001$, ** $p < 0.01$. (e) Western blotting analysis with an anti-human MMP-12 antibody was performed for the supernatants from cultured NHDFs. The obtained bands of the active form of MMP-12 were analyzed using a densitometer and the values in the graph are represented relatively. The values reported represent means \pm SD. * $p < 0.05$. (f) NHDFs were cultured for 8 days with or without 20 nM human recombinant MFAP-4 during the culture in FBS-free medium. Immunofluorescence staining was performed as described in the legend of Fig. 5c. Scale bars = 50 μ m.

suggesting that MFAP-4 is in charge of the direct interaction with fibrillin-1 for the promotion of microfibril assembly.

MFAP-4 over-expression prevents UVB-induced collagen degradation as well as elastin deterioration. Given that the expression of pro-MMP-1 is induced by elastin peptides in skin fibroblasts^{41,42}, the finding of the role of MFAP-4 in the promotion of elastic fiber assembly prompted us to also investigate its impact on the metabolism of collagen I. Immunohistochemical analysis with an anti-human collagen I antibody demonstrated that collagen I localisation was observed throughout the dermis in the control reporter gene-transfected skin without UVB exposure but was markedly degraded after UVB exposure for 8 wks (Fig. 7a). In contrast, the deposited collagen I in skin treated with a lentiviral vector encoding MFAP-4 was protected from UVB-induced degradation. In agreement with those immunohistochemical analyses, Western blotting analysis also showed that collagen I abundance in skin over-expressing *MFAP-4* was higher than in skin over-expressing a control reporter gene before and after repeated UVB irradiation for 4 wks (Fig. 7b). Subsequently, further confirmation of the impact of MFAP-4 deficiency on MMP-1 expression was examined using NHDFs. NHDFs treated with a non-specific siRNA in the presence or absence of human recombinant MFAP-4 or NHDFs treated with a siRNA specific for MFAP-4 were cultured for 8 days. The expression of MMP-1 transcripts was significantly increased in NHDFs with impaired

expression of MFAP-4 (Fig. 7c). Consistently, the secretion of active MMP-1 was also stimulated when MFAP-4 expression was knocked down (Fig. 7d).

Discussion

Elasticity provided by elastic fiber formation is essential to maintain tissue flexibility and extensibility for many organs such as the large arteries, lungs, and skin³⁰. Although fibrillin-1 microfibrils and tropoelastin protein represent the majority of elastic fiber components, it has been poorly understood how microfibrils are built following fibrillin-1 assembly and how microfibrils and tropoelastin interact during elastic fiber organization. Recently, it was shown that a disintegrin and metalloproteinase with thrombospondin motifs-like-6 protein directly binds to fibrillin-1 to promote the formation of fibrillin-1 microfibrils⁴³. Another recent study revealed that fibulin-4 protein is indispensable for tethering LOX to tropoelastin to facilitate cross-linking⁴⁴. Those reports are of great importance to comprehend the mechanisms underlying the construction of elastic fibers, whereas it remains to be determined how many other molecules are involved in elastogenesis to completely understand the process of elastic fiber formation. For example, MAGP-36, a homologue of MFAP-4 detected around elastic fibers in various animals, was reported to have disappeared in photoaged dermis but accumulated in disintegrated elastic fibers in the lesional skin of pseudoxanthoma elasticum, an elastin-related disorder⁴⁰. These findings encouraged us to explore the function of MFAP-4 in human skin

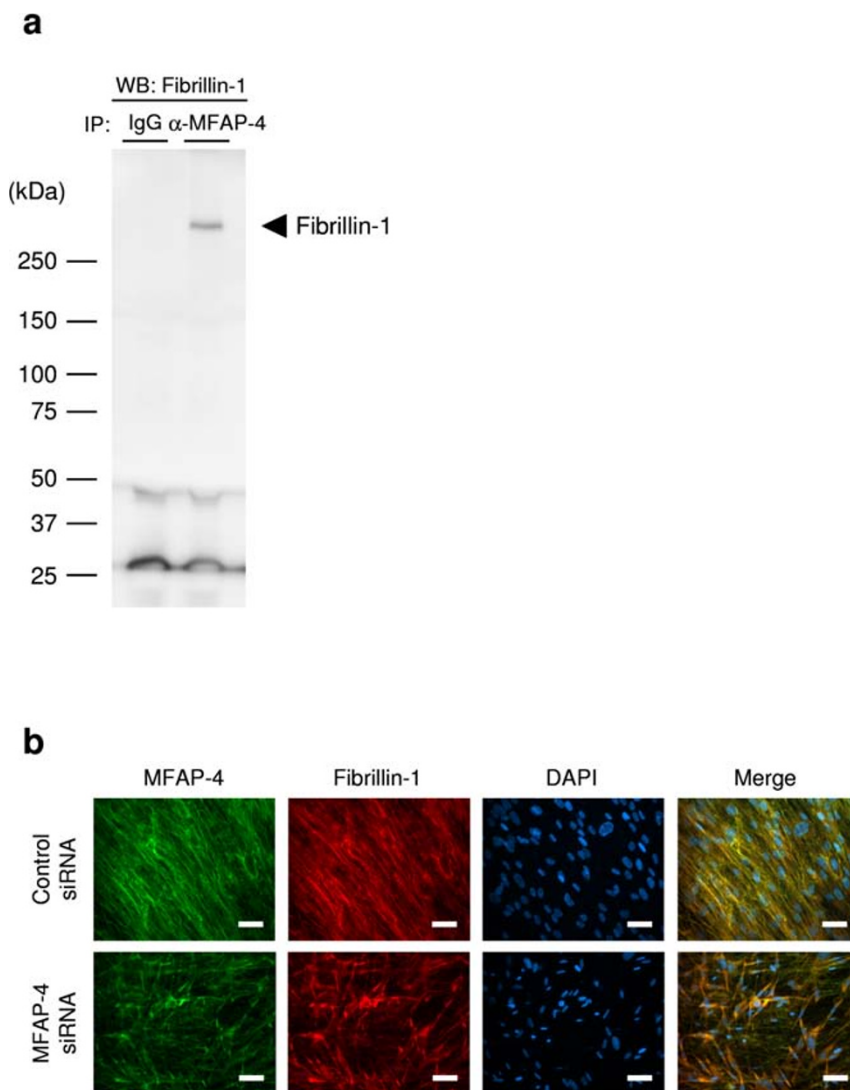


Figure 6 | MFAP-4 directly interacts with fibrillin-1 to form microfibrils. (a) Concentrated supernatants from NHDFs cultured for 8 days were immunoprecipitated with an anti-MFAP-4 antibody or normal rabbit IgG. Immunoprecipitants were analyzed by Western blotting with an anti-fibrillin-1 antibody. (b) NHDFs were transfected with siRNAs for non-specific sequences (Control) or MFAP-4 twice during the culture for 8 days, followed by immunofluorescence staining with an anti-human MFAP-4 antibody (green) and an anti-human fibrillin-1 antibody (red). Nuclear staining (DAPI) and merged images are also shown. Scale bars = 50 μ m.

using an *in vivo* photodamaged/photoaged skin model with human skin xenografted on SCID mice in concert with a lentiviral vector to over-express MFAP-4 as well as *in vitro* NHDFs combined with siRNA technology.

One of the most significant problems that needed to be addressed in this study was the consideration of how MFAP-4 is involved in elastic fiber formation. It has been previously demonstrated that fibulin-4 and -5 are in charge of recruiting tropoelastins and its cross-linking enzymes onto microfibrils in order to accelerate elastic fiber assembly in collaboration with LTBP-2, which binds to heparin and heparin sulfate proteoglycans^{45–49}. In addition, the abundance of fibulin-5 has also been documented to be decreased both in photoaged and in intrinsically aged dermis, suggesting that it plays a role in maintaining cutaneous elasticity⁵⁰. Given that fibulins play roles in the assembly and cross-linking of tropoelastin monomers, it is reasonable to hypothesize that MFAP-4 contributes to the development of microfibrils rather than the tethering of LOX to tropoelastin which is mainly regulated by fibulins. We have clearly demonstrated that MFAP-4 interacts with fibrillin-1, whose production is also reported to be decreased in photoaged skin⁵¹, and not with

tropoelastin for the organization of microfibrils which allows the participation of tropoelastin cross-linked with LOX for the formation of functional mature elastic fibers substantially required for skin homeostasis. Based on our findings, we propose a model for the contribution of MFAP-4 to the development of elastic fibers (Fig. 8). By virtue of the presence of MFAP-4, fibrillin-1 can be assembled to form microfibrils followed by the cross-linking of tropoelastins tethered with LOX to microfibrils, as supported by a previous study⁴⁴. In addition to its role in the development of microfibrils, another important role of MFAP-4 in the suppression of MMP-12 activity is illustrated both in our *in vivo* and *in vitro* analyses. In parallel with previous studies indicating that elastin-derived peptides induce the expression of various kinds of MMPs (including MMP-12) in several types of cells^{52,53} and that UV radiation alone is sufficient to selectively degrade many elastic fiber associated proteins⁵⁴, the enhancement of MFAP-4 is thought to be in charge of the suppression of MMP-12 activity as well as the promotion of microfibril formation which is essential for the organization of functional elastic fibers, resulting in the observed photoprotection.

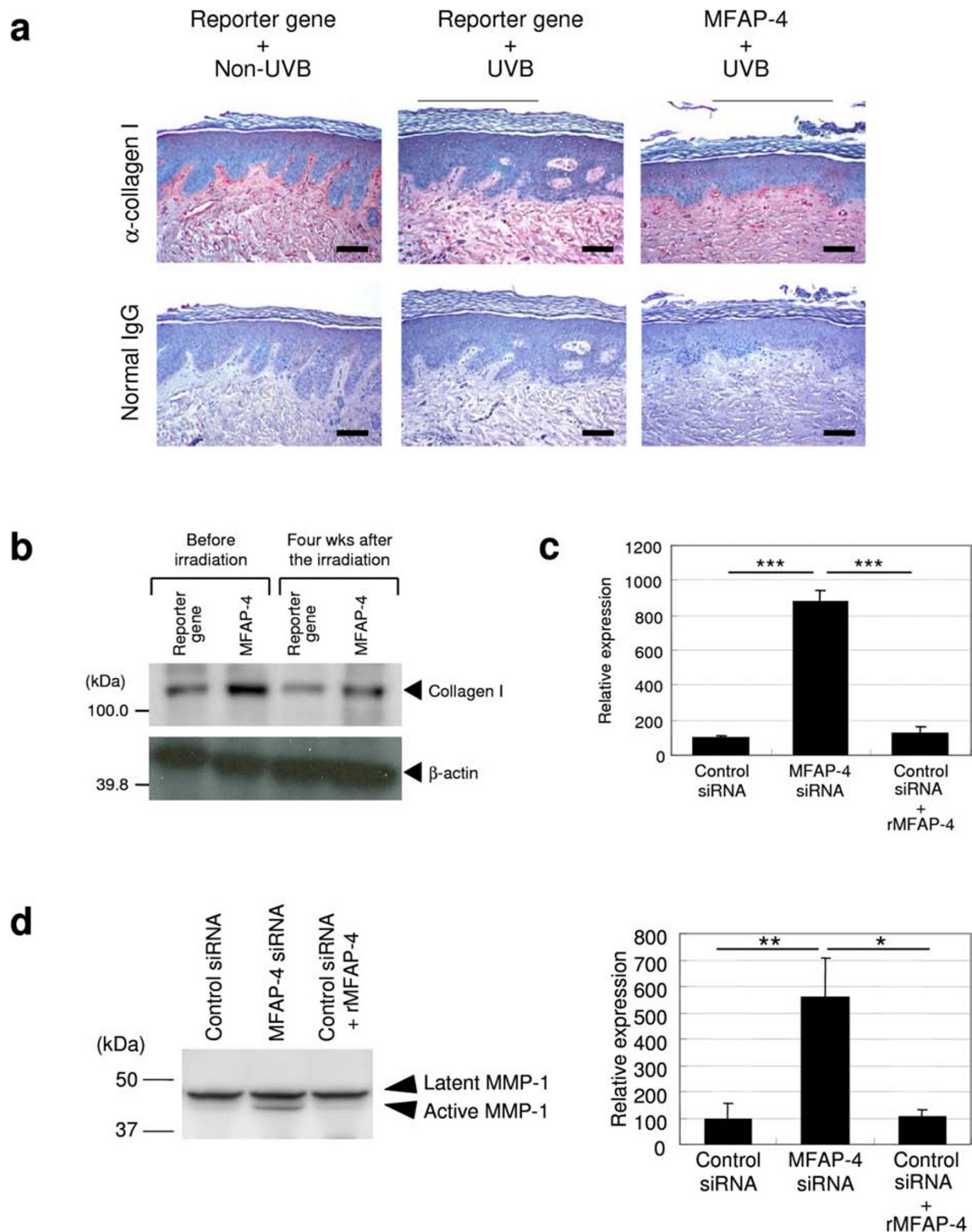


Figure 7 | MFAP-4 over-expression prevents UVB-induced deterioration of collagen I. (a) Immunohistochemical analysis with a rabbit anti-human collagen I antibody or a non-specific control rabbit IgG was carried out using paraffin embedded sections from the xenografted skin treated with a lentiviral vector encoding a control reporter gene with or without continuous UVB irradiation for 8 wks and using xenografted skin over-expressing *MFAP-4* with UVB exposure for 8 wks. Scale bars = 100 μ m. (b) Western blotting analysis with an anti-human collagen I or an anti-human β -actin antibody to assess the protein levels of collagen I in xenografted skin treated with lentiviral vectors encoding a control reporter gene or *MFAP-4* before and after UVB exposure for 4 wks. (c) NHDFs were transfected with siRNAs for non-specific sequences (Control) or *MFAP-4* twice during the culture for 8 days. Control siRNA-transfected cells were treated with or without 10 nM human recombinant *MFAP-4* during the culture. Quantitative RT-PCR analysis of the *MMP-1* mRNA expression in cultured NHDFs was performed as described in the legend of Fig. 5a. The values reported represent means \pm SD. *** p <0.001. (d) Western blotting analysis with an anti-human *MMP-1* antibody was conducted for supernatants from cultured NHDFs treated as described in Fig. 7c. The obtained bands of the active form of *MMP-1* were analyzed using a densitometer and the values in the graph are represented relatively. The values reported represent means \pm SD. ** p <0.01, * p <0.05.

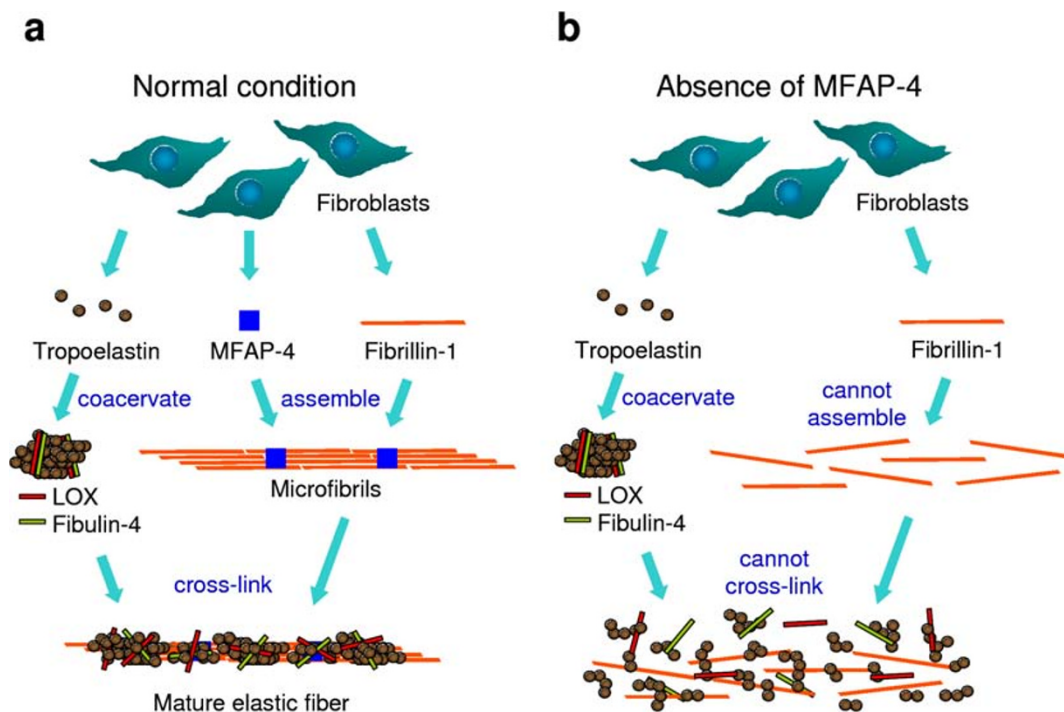


Figure 8 | Schematic representation of the role of MFAP-4 in elastic fiber formation. (a) Secreted MFAP-4 and fibrillin-1 interact directly, resulting in the assembly of microfibrils under normal conditions. Tropoelastins assembled with LOX recruited by fibulin-4 are subsequently cross-linked with microfibrils for the formation of complete mature elastic fibers. (b) In the absence of MFAP-4, fibrillin-1 cannot be assembled or matured for the formation of microfibrils. Tropoelastins are never cross-linked due to the failure of microfibril formation.

It is also of interest to investigate the impact of the elastic fiber formation mediated by MFAP-4 on another major type of age-dependent-decreasing components, collagens, because it has been reported that MAGP-36 also binds to collagen I³⁹. Our data indicate that over-expression of MFAP-4 protects against UVB-induced degradation of collagen I which is associated with the inhibition of photodamage/photoaging deterioration in xenografted human skin *in vivo*. Further, the amount of MMP-1, which is one of the collagenases expressed by dermal fibroblasts³⁵, was significantly up-regulated in MFAP-4 knockdown NHDFs both at the transcript and the protein levels. Consistently, elevation of MMP-1 in dermal fibroblasts is also observed when the cells are exposed to broken collagens in organ cultures of human skin³⁶. These findings led us to hypothesize that MFAP-4 has another role in the stabilization of collagen I. Given that the expression of pro-MMP-1 is stimulated by elastin peptides in skin fibroblasts^{41,42}, it is reasonable to propose another role of MFAP-4 in the maintenance of collagens which is also important for skin homeostasis. In addition to the protection of collagen I by increased MFAP-4 expression, UVB-induced deterioration of collagen IV was also found to be hindered in our photodamage model of xenografted human skin (data not shown).

In conclusion, our data reveal for the first time that the protein levels of MFAP-4 are decreased both in extrinsic photoaged skin and in intrinsic aged skins, and that the enhancement of MFAP-4 expression protects the skin from UVB-induced photodamage/photoaging characterized by the degradation of fibers of elastin and collagens resulting in the aggravation of skin elasticity. More importantly, MFAP-4 plays essential roles not only in microfibril development by direct interaction with fibrillin-1 but also in the maintenance of ECM proteins, including collagen I, by an as yet undisclosed mechanism(s). These findings provide new insights into a fundamental comprehension of the mechanisms underlying microfibril formation resulting in skin homeostasis and also achieve a basis to develop an efficient strategy for treating UV-induced skin disorders.

Methods

Human skin. Full-thickness abdominal skin from a healthy 41-year-old Caucasian female with type II skin undergoing abdominoplasty and breast skin from a healthy 46-year-old Caucasian female with type II skin undergoing breast reduction (University Pointe, Cincinnati, OH, USA), were used for skin xenografts. Three to four punch biopsies of skin at the ventral upper arm or the dorsal lower arm from healthy Caucasian females with type II skin in their twenties, thirties, fifties and sixties (Stephens and Associates, Carrollton, TX, USA) were also used for the investigation of mRNA transcript expression or protein localisation. Collection of the specimens was approved by the Institutional Review Board of the Cincinnati Children's Hospital Medical Center or the IntegReview Ethical Review Board (Austin, TX) and informed consent was obtained from the volunteers prior to the procedure.

Animal grafting. Sixty female ICR-SCID mice, 4 to 6 wks old (Taconic Farms, Germantown, NY) were handled according to the guidelines of the Institutional Animal Care and Use Committee at Cincinnati Children's Hospital that approved the experiments and were kept under pathogen-free conditions throughout the experiments. Full-thickness abdominal and breast skins were xenografted onto SCID mice anesthetized and maintained using isoflurane/oxygen (2%/0.7L) throughout the surgery as described previously¹⁶. Briefly, after the dorsal skin of each mouse was cut to produce a wound bed approximately 2.0 to 3.0 cm in diameter, the full-thickness human skin was sutured in place with a reverse cutting precision monofilament PS-3, 6-0. Sensorcaine was applied to the graft bed edges to provide analgesia.

UVB exposure. Chronic UVB exposure of the human skin xenografted onto SCID mice was started approximately 10 wks after the grafting when healing was complete, as previously described¹. Briefly, a bank of two UVB lamps (340044-1 lamps; UVB, Upland, CA) with a filter yielding an emission peak near 302 nm was used, and the energy output was measured using a UV light meter, UV-340 MSR7000 (Lutron Electronic Enterprise Co., Ltd., Taipei, Taiwan). A progressive UVB exposure regimen was used starting at 40 mJ/cm² (1 minimal erythema dose; MED) and was increased by 10 mJ/cm² per week until week 3. The irradiation dose of 60 mJ/cm² was then kept constant for the remaining period of exposure. The grafted human skin was irradiated 5 times weekly for 6 or 8 wks yielding total UVB doses of approximately 1.65 or 2.2 J/cm², respectively. Before or after each UVB exposure, a 30 sec mechanical stretching was applied to stimulate the physiological movement of human skin.

Lentiviral vector design. Full length MFAP-4 was prepared from a skin cDNA library (Invitrogen, Carlsbad, CA) using the following primer sets.

MFAP-4-5': ATA-TAT-CTA-GAG-CCA-CCA-TGA-AGG-CAC-TCC-TGG-CC
MFAP-4-3': TAT-AAG-GCC-TTG-GCC-CGG-ATT-TTC-AT



The amplified PCR product was treated with Klenow enzyme before being cut with XbaI, and was then cloned as a half-blunted fragment into pBlueScript at the XbaI/SmaI sites. After the isolation of plasmid DNA, MFAP-4 in pBlueScript was released using StuI and XbaI and was then cloned into DeltaUX3M-9. Finally, the helper packaging construct pCMVR8.2, the transfer vector DeltaUX3M-9-MFAP-4, and a plasmid encoding vesicular stomatitis virus glycoprotein (VSV-G) were used for triple transfection as described elsewhere⁵⁷. The transfer vectors DeltaUX3M-9-eGFP and DeltaUX3M-9- β -galactosidase were also prepared for reporter gene-expressing vectors and their titers were examined as described previously⁵⁸.

Over-expression of MFAP-4 in xenografted human skin. After the certification of viral stocks to be RCL-free, approximately 25 μ l VSV-G pseudotyped lentiviral vector encoding MFAP-4 or reporter genes (1.5×10^9 TU/ml) was intradermally injected into the completely healed human skin xenografted onto SCID mice twice with a week interval as described elsewhere⁵⁹.

Skin profilometric measurement. Replicas of skin xenografts were prepared using the replica agent SILFLO (Flexico Developments, Potters Bar, UK) at the indicated points as described elsewhere¹⁶. In brief, skin replicas compressed using GC exafine (GC Corporation, Tokyo, Japan) were analyzed by the use of 3-dimensional optical measurement of each replica using PRIMOS Compact (GF Messtechnik GmbH, Berlin, Germany) as reported previously¹⁶. After the measurement, moiré fringes were eliminated and a rectangular area (4 to 5 mm \times 7 to 9 mm) was chosen in the central part of each replica in a plane analysis. Two 2-dimensional parameters, Sa and Sz, were used to assess the degree of photodamage. Sa is the average of absolute values of the area of mountains and of valleys reflecting wrinkles per certain area and Sz represents the arithmetical average of maximum peak to valley height of the roughness values of 5 consecutive sampling sections over the filtered profile.

Elasticity assessment. Skin elasticity was analyzed using the Cutometer SEM575 (Courage & Khazaka Electronic, Köln, Germany) as previously documented⁶⁰. Briefly, the center of each skin xenograft was used for 5 seconds application loads of 200 hPa, followed by a 2 seconds relaxation period. Two parameters, Ue (the immediate deformation) and Ur (the immediate refraction), were used as indicators of elasticity degree. Ur/Ue = pure elasticity ignoring creep.

MMP-12 activity assay. Whole skin was solubilized for MMP-12 activity measurement using a SensoLyte™ 520 MMP-12 Fluorimetric Assay Kit (AnaSpec Corporate, San Jose, CA).

Cell culture. NHDFs (Kurabo Corporation, Osaka, Japan) were maintained in Dulbecco's modified Eagle's medium (Invitrogen) containing 5% (v/v) fetal bovine serum (FBS) at 37°C in a humidified atmosphere containing 5% CO₂.

siRNA transfection. NHDFs seeded on a cover glass in a cell culture plate were transfected using siRNA (a non-specific sequence for a control or a specific sequence for MFAP-4) and Lipofectamine 2000 reagent (Invitrogen) twice with 96 hours interval according to the manufacturer's instructions. Supernatants and cells were collected for Western blotting analysis and immunocytochemical and real-time quantitative RT-PCR analyses, respectively, 72 hours after the second transfection.

Immunocytochemical analysis. NHDFs, fixed in ice-cold methanol and subsequently treated for non-specific immunoreactivity blocking, were incubated with diluted rabbit anti-human tropoelastin antibody (Elastin Products Company, Owensville, MO), rabbit anti-human MFAP-4 antibody or mouse anti-human fibrillin-1 antibody (Millipore, Billerica, MA), and subsequently with diluted Alexa Fluor 488-labeled anti rabbit IgG antibody or Alexa Fluor 546-labeled anti mouse IgG antibody. The cells attached to the cover glass were mounted on a slide glass using ProLong Gold antifade reagent with DAPI (Invitrogen), and immunoreactivity was observed using a Leica DMR fluorescence microscope (Leica Microsystems GmbH, Wetzlar, Germany).

Real-time RT-PCR analysis. Using real-time quantitative RT-PCR normalized against the expression of ribosomal protein large P0 (*RPLP0*) or glyceraldehyde-3-phosphate dehydrogenase (*GAPDH*), the transcript expression of MFAP-4, MMP-12 or MMP-1 was determined in xenografted human skin 24 hours after the repetitive UVB exposure for 6 wks and in biopsied skin specimens from the ventral upper arms of young (20's) and old (50's) donors collected in RNAlater (Qiagen, Valencia, CA). Total RNAs from each skin sample and from siRNA-transfected NHDFs were prepared using a RNeasy micro kit (Qiagen). cDNAs were synthesized by reverse transcription of total RNA using oligo dT and Moloney murine leukemia virus reverse transcriptase. Real-time quantitative RT-PCRs with TaqMan gene expression assays (Applied Biosystems, Foster City, CA, USA) were performed using an ABI Prism 7300 or 7500 sequence detection system (Applied Biosystems).

Immunoprecipitation. Supernatants from cultured NHDFs were concentrated using a 3 kDa-cut off membrane (Millipore), followed by the incubation with anti-human MFAP-4 antibody (AdipoGen, Incheon, Korea) or normal rabbit IgG. Protein G Sepharose beads (GE Healthcare, Waukesha, WI) were then added to the mixture and incubated before the collection of the beads by centrifugation. Immunoprecipitated proteins were suspended in 1X SDS sample buffer (Thermo Fisher scientific, Waltham, MA) for Western blotting analysis.

Western blotting analysis. Xenografted skin samples were lysed in cell lysis buffer (Cell Signaling Technology, Danvers, MA) containing 1 mM phenylmethylsulfonyl fluoride (Sigma, St. Louis, MO). Twenty μ g of each tissue extract or 12 μ l of each culture medium from NHDFs were separated on 7.5% or 12% SDS gels (Bio-Rad Laboratories, Hercules, CA). Samples were transferred to PVDF membranes (Bio-Rad Laboratories) and were incubated with antibodies specific for human MFAP-4 (AdipoGen, Incheon, Korea), human collagen I (United States Biological, Swampscott, MA), human MMP-1 (AbD Serotec, Oxford, UK), human MMP-12 (Millipore), human fibrillin-1 (Elastin Products Company) or human β -actin (Sigma). Subsequent visualization of antibody recognition was performed using Enhanced Chemiluminescence Plus (GE Healthcare) according to the manufacturer's instructions.

Immunohistochemistry. Xenografted human skins and punch biopsy-derived human skins from the subjects in their thirties and sixties were fixed in 10% buffered formalin and embedded in paraffin. The immunoreactivities of MFAP-4 and collagen I were assessed using anti-human MFAP-4 (Abcam, Cambridge, UK) and anti-human collagen I (United States Biological), respectively, as described elsewhere¹⁶. Normal rabbit IgG was used as a negative control. The immunoreactivity of MFAP-4 and collagen I were visualized using a CSAII biotin-free catalyzed signal amplification system (DAKO) with aminoethylcarbazole.

Luna staining. Five μ m thick sections of xenografted human skin were stained using conventional Luna staining for the visualization of fine elastic fibers.

Statistics. The level of significance of differences among the groups was analyzed using Student *t*-test. Differences in the mean or raw values among the groups were considered significant when $p < 0.05$.

1. Crutzen, P. J. Ultraviolet on the increase. *Nature* **356**, 104–105 (1992).
2. Slaper, H., Velders, G. J. M., Daniel, J. S., De, Gruijl, F. R. & Van der, Leun, J. C. Estimates of ozone depletion and skin cancer incidence to examine the Vienna Convention achievements. *Nature* **384**, 256–258 (1996).
3. Scharfetter-Kochanek, K. *et al.* UV-induced reactive oxygen species in photocarcinogenesis and photoaging. *Biol. Chem.* **378**, 1247–1257 (1997).
4. Nakagawa, H. Cutaneous aging processes. *J. Japanese Cosmetic Science Society* **24**, 120–123 (2000).
5. Braverman, I. M. & Fonferko, E. Studies in cutaneous aging: 1. The elastic fiber network. *J. Invest. Dermatol.* **78**, 434–443 (1982).
6. Uitto, J. Connective tissue biochemistry of aging dermis. Age-related alterations in collagen and elastin. *Dermatol. Clin.* **4**, 433–446 (1986).
7. Schwartz, E. Connective tissue alterations in the skin of ultraviolet irradiated hairless mice. *J. Invest. Dermatol.* **91**, 158–161 (1988).
8. Zheng, P. & Kligman, L. H. UVA-induced ultrastructural changes in hairless mouse skin: a comparison to UVB-induced damage. *J. Invest. Dermatol.* **100**, 194–199 (1993).
9. Bernstein, E. F. *et al.* Enhanced elastin and fibrillin gene expression in chronically photodamaged skin. *J. Invest. Dermatol.* **103**, 182–186 (1994).
10. Schwartz, E., Feinberg, E., Lebowitz, M., Mariani, T. J. & Boyd, C. D. Ultraviolet radiation increases tropoelastin accumulation by a post-transcriptional mechanism in dermal fibroblasts. *J. Invest. Dermatol.* **105**, 65–69 (1995).
11. Bernstein, E. F. & Uitto, J. The effect of photodamage on dermal extracellular matrix. *Clin. Dermatol.* **14**, 143–151 (1996).
12. Starcher, B., Pierce, R. & Hinek, A. UVB irradiation stimulates deposition of new elastic fibers by modified epithelial cells surrounding the hair follicles and sebaceous glands in mice. *J. Invest. Dermatol.* **112**, 450–455 (1999).
13. Kambayashi, H. *et al.* Epidermal changes caused by chronic low-dose UV irradiation induce wrinkle formation in hairless mouse. *J. Dermatol. Sci.* **27**, S19–S25 (2001).
14. Kambayashi, H., Odake, Y., Takada, K., Funasaka, Y. & Ichihashi, M. Involvement of changes in stratum corneum keratin in wrinkle formation by chronic ultraviolet irradiation in hairless mice. *Exp. Dermatol.* **12**, 22–27 (2003).
15. Sano, T. *et al.* The formation of wrinkles caused by transition of keratin intermediate filaments after repetitive UVB exposure. *Arch. Dermatol. Res.* **296**, 359–365 (2005).
16. Hachiya, A. *et al.* Mechanistic effects of long-term ultraviolet B irradiation induce epidermal and dermal changes in human skin xenografts. *Am. J. Pathol.* **174**, 401–413 (2009).
17. Oxlund, H., Manscho, J. & Viidik, A. The role of elastin in the mechanical properties of skin. *J. Biomech.* **21**, 213–218 (1988).
18. Imayama, S. & Braverman, I. M. A hypothetical explanation for the aging of skin. Chronologic alteration of the three-dimensional arrangement of collagen and elastic fibers in connective tissue. *Am. J. Pathol.* **134**, 1019–1025 (1989).
19. Labat-Robert, J., Fourtanier, A., Boyer-Lafargue, B. & Robert, L. Age dependent increase of elastase type protease activity in mouse skin. Effect of UV-irradiation. *J. Photochem. Photobiol. B.* **57**, 113–118 (2000).
20. Tsukahara, K. *et al.* Selective inhibition of skin fibroblast elastase elicits a concentration-dependent prevention of ultraviolet B-induced wrinkle formation. *J. Invest. Dermatol.* **117**, 671–677 (2001).



21. Tsuji, N., Moriwaki, S., Suzuki, Y., Takema, Y. & Imokawa, G. The role of elastases secreted by fibroblasts in wrinkle formation: implication through selective inhibition of elastase activity. *Photochem. Photobiol.* **74**, 283–290 (2001).
22. Chung, J. H. *et al.* Ultraviolet modulation of human macrophage metalloelastase in human skin in vivo. *J. Invest. Dermatol.* **119**, 507–512 (2002).
23. Mera, S. L., Lovell, C. R., Jones, R. R. & Davies, J. D. Elastic fibres in normal and sun-damaged skin: an immunohistochemical study. *Br. J. Dermatol.* **117**, 21–27 (1987).
24. Montagna, W., Kirchner, S. & Carlisle, K. Histology of sun-damaged human skin. *J. Am. Acad. Dermatol.* **21**, 907–918 (1989).
25. Warren, R. *et al.* Age, sunlight, and facial skin: a histologic and quantitative study. *J. Am. Acad. Dermatol.* **25**, 751–760 (1991).
26. Seo, J. Y. *et al.* Ultraviolet radiation increases tropoelastin mRNA expression in the epidermis of human skin in vivo. *J. Invest. Dermatol.* **116**, 915–919 (2001).
27. Sakai, L. Y., Keene, D. R. & Engvall, E. Fibrillin, A new 350-kD glycoprotein, is a component of extracellular microfibrils. *J. Cell Biol.* **103**, 2499–2509 (1986).
28. Hollister, D. W., Godfrey, M., Sakai, L. Y. & Pyeritz, R. E. Immunohistologic abnormalities of the microfibrillar-fiber system in the Marfan syndrome. *N. Engl. J. Med.* **323**, 152–159 (1990).
29. Kiely, C. M., Sherratt, M. J. & Shuttleworth, C. A. Elastic fibres. *J. Cell Sci.* **115**, 2817–2828 (2002).
30. Wagenseil, J. E. & Mecham, R. P. New insights into elastic fiber assembly. *Birth Defects Res. C.* **81**, 229–240 (2007).
31. Gray, W. R., Sandberg, L. B. & Foster, J. A. Molecular model for elastin structure and function. *Nature* **246**, 461–466 (1973).
32. Narayanan, A. S., Page, R. C., Kuzan, F. & Cooper, C. G. Elastin cross-linking in vitro. Studies on factors influencing the formation of desmosines by lysyl oxidase action on tropoelastin. *Biochem. J.* **173**, 857–862 (1978).
33. Bellingham, C. M., Woodhouse, K. A., Robson, P., Rothstein, S. J. & Keeley, F. W. Self-aggregation characteristics of recombinantly expressed human elastin polypeptides. *Biochim. Biophys. Acta.* **1550**, 6–19 (2001).
34. Toonkool, P., Jensen, S. A., Maxwell, A. L. & Weiss, A. S. Hydrophobic domains of human tropoelastin interact in a context-dependent manner. *J. Biol. Chem.* **276**, 44575–44580 (2001).
35. Zhao, Z. *et al.* The gene for a human microfibril-associated glycoprotein is commonly deleted in Smith-Magenis syndrome patients. *Hum. Mol. Genet.* **4**, 589–597 (1995).
36. Kobayashi, R. *et al.* Isolation and characterization of a new 36-kDa microfibril-associated glycoprotein from porcine aorta. *J. Biol. Chem.* **264**, 17437–17444 (1989).
37. Kobayashi, R., Mizutani, A. & Hidaka, H. Isolation and characterization of a 36-kDa microfibril-associated glycoprotein by the newly synthesized isoquinolinesulfonamide affinity chromatography. *Biochem. Biophys. Res. Commun.* **198**, 1262–1266 (1994).
38. Toyoshima, T. *et al.* Ultrastructural distribution of 36-kD microfibril-associated glycoprotein (MAGP-36) in human and bovine tissues. *J. Histochem. Cytochem.* **47**, 1049–1056 (1999).
39. Toyoshima, T., Nishi, N., Kusama, H., Kobayashi, R. & Itano, T. 36-kDa microfibril-associated glycoprotein (MAGP-36) is an elastin-binding protein increased in chick aortae during development and growth. *Exp. Cell. Res.* **307**, 224–230 (2005).
40. Hirano, E. *et al.* Expression of 36-kDa microfibril-associated glycoprotein (MAGP-36) in human keratinocytes and its localization in skin. *J. Dermatol. Sci.* **28**, 60–67 (2002).
41. Brassart, B. *et al.* Conformational dependence of collagenase (matrix metalloproteinase-1) up-regulation by elastin peptides in cultured fibroblasts. *J. Biol. Chem.* **276**, 5222–5227 (2001).
42. Duca, L. *et al.* The elastin receptor complex transduces signals through the catalytic activity of its Neu-1 subunit. *J. Biol. Chem.* **282**, 12484–12491 (2007).
43. Tsutsui, K. *et al.* ADAMTSL-6 is a novel extracellular matrix protein that binds to fibrillin-1 and promotes fibrillin-1 fibril formation. *J. Biol. Chem.* **285**, 4870–4882 (2010).
44. Horiguchi, M. *et al.* Fibulin-4 conducts proper elastogenesis via interaction with cross-linking enzyme lysyl oxidase. *Proc. Natl. Acad. Sci. USA* **106**, 19029–19034 (2009).
45. Nakamura, T. *et al.* Fibulin-5/DANCE is essential for elastogenesis in vivo. *Nature* **415**, 171–175 (2002).
46. Hirai, M. *et al.* Latent TGF-beta-binding protein 2 binds to DANCE/fibulin-5 and regulates elastic fiber assembly. *EMBO J.* **26**, 3283–3295 (2007).
47. Katsuta, Y. *et al.* Fibulin-5 accelerates elastic fibre assembly in human skin fibroblasts. *Exp. Dermatol.* **17**, 837–842 (2008).
48. Choudhury, R. *et al.* Differential regulation of elastic fiber formation by fibulin-4 and -5. *J. Biol. Chem.* **284**, 24553–24567 (2009).
49. Parsi, M. K., Adams, J. R., Whitelock, J. & Gibson, M. A. LTBP-2 has multiple heparin/heparan sulfate binding sites. *Matrix Biol.* **29**, 393–401 (2010).
50. Kadoya, K. *et al.* Fibulin-5 deposition in human skin: decrease with ageing and ultraviolet B exposure and increase in solar elastosis. *Br. J. Dermatol.* **153**, 607–612 (2005).
51. Watson, R. E. *et al.* Fibrillin-rich microfibrils are reduced in photoaged skin. Distribution at the dermal-epidermal junction. *J. Invest. Dermatol.* **112**, 782–787 (1999).
52. Coquerel, B. *et al.* Elastin-derived peptides: matrikines critical for glioblastoma cell aggressiveness in a 3-D system. *Glia* **57**, 1716–1726 (2009).
53. Park, J. B., Kong, C. G., Suhl, K. H., Chang, E. D. & Riew, K. D. The increased expression of matrix metalloproteinases associated with elastin degradation and fibrosis of the ligamentum flavum in patients with lumbar spinal stenosis. *Clin. Orthop. Surg.* **1**, 81–89 (2009).
54. Sherratt, M. J. *et al.* Low-dose ultraviolet radiation selectively degrades chromophore-rich extracellular matrix components. *J. Pathol.* **222**, 32–40 (2010).
55. Moon, S. E., Dame, M. K., Remick, D. R., Elder, J. T. & Varani, J. Induction of matrix metalloproteinase-1 (MMP-1) during epidermal invasion of the stroma in human skin organ culture: keratinocyte stimulation of fibroblast MMP-1 production. *Br. J. Cancer.* **85**, 1600–1605 (2001).
56. Fisher, G. J. *et al.* Collagen fragmentation promotes oxidative stress and elevates matrix metalloproteinase-1 in fibroblasts in aged human skin. *Am. J. Pathol.* **174**, 101–114 (2009).
57. Watson, D. J., Kobinger, G. P., Passini, M. A., Wilson, J. M. & Wolfe, J. H. Targeted transduction patterns in the mouse brain by lentivirus vectors pseudotyped with VSV, Ebola, Mokola, LCMV, or MuLV envelope proteins. *Mol. Ther.* **5**, 528–537 (2002).
58. Croyle, M. A. *et al.* PEGylation of a vesicular stomatitis virus G pseudotyped lentivirus vector prevents inactivation in serum. *J. Virol.* **78**, 912–921 (2004).
59. Hachiya, A. *et al.* Gene transfer in human skin with different pseudotyped HIV-based vectors. *Gene Ther.* **14**, 648–656 (2007).
60. Takema, Y., Yorimoto, Y., Kawai, M. & Imokawa, G. Age-related changes in the elastic properties and thickness of human facial skin. *Br. J. Dermatol.* **131**, 641–648 (1994).

Acknowledgements

We thank Dr. Jun Yang (Key Clone Technologies) for technical expertise in plasmid modification and for critical discussions of vector design and Ms. Megan Kanski for her assistance with the maintenance of human skins xenografted onto SCID mice.

Author contributions

The author(s) have made the following declarations about their contributions: Conceived and designed the experiments: SK, AH. Performed the experiments: SK, AH, PS, KH. Analyzed the data: AH. Made the virus vectors: AB, GPK. Wrote the paper: SK, AH, GPK. Supervised the research: TF, MOV, WJK, TK, YT.

Additional information

Competing financial interests: The authors declare no competing financial interests.

License: This work is licensed under a Creative Commons Attribution-NonCommercial-ShareAlike 3.0 Unported License. To view a copy of this license, visit <http://creativecommons.org/licenses/by-nc-sa/3.0/>

How to cite this article: Kasamatsu, S. *et al.* Essential role of microfibrillar-associated protein 4 in human cutaneous homeostasis and in its photoprotection. *Sci. Rep.* **1**, 164; DOI:10.1038/srep00164 (2011).